

## Stripping Distortions in $B^{11}(d,p\gamma)B^{12}_{0.95}$ Angular Correlations\*

A. P. BORDEN† AND R. C. RITTER

University of Virginia, Charlottesville, Virginia

(Received 23 February 1967)

$p$ - $\gamma$  angular correlations were measured in the  $B^{11}(d,p\gamma)B^{12}_{0.95}$  reaction in order to determine how its distortions depend on deuteron energy and proton angle. Various proton angles were used, with  $E_d=1.0, 1.8, 3.0,$  and  $5.5$  MeV. These parameters were chosen to systematically test predictions based on an application of the dispersion theory of direct nuclear reactions. The observed failure of the correlation anisotropy to increase as the stripping denominator  $D$  is reduced is most easily interpreted as a negative result for the application of this concept to the  $B^{11}(d,p)B^{12}_{0.95}$  reaction. Trends in the behavior of the data are discussed. In addition, spectroscopic information about the captured neutron is deduced, and the excited state of  $B^{12}$  is compared with shell-model theory.

### I. INTRODUCTION

IT is of interest to pursue an understanding of nuclear-stripping reactions through relatively simple concepts which illuminate systematics or trends rather than detailed structure. An effort of this type has been initiated by Wilkinson.<sup>1</sup> He pointed out that low-energy, low- $Q$ -value deuteron stripping reactions might be relatively undistorted. Interest in the possible validity of such a simplifying circumstance has prompted a number of experimental tests employing angular distribution measurements. Some of these tests have been evaluated<sup>2,3</sup> in the context of a theory based on dispersion relations<sup>4</sup> which restates Wilkinson's concept in terms of a parameter  $D$ , the distance to the stripping pole. As predicted by this theory, the fit of the angular distributions to plane-wave Born approximation (PWBA) (PWBA is here considered synonymous with Butler theory where cutoff radial integration is employed. Unless stated otherwise, a good PWBA or Butler fit means only that the angular dependence of the distribution is accounted for) theory was found, in the cases studied, to systematically extend to larger angles with decreasing deuteron energy.

Such apparently positive results have not been definitive because of ambiguity in interpretation. Deuteron stripping angular distributions usually become relatively broad and simple at low bombarding energies and are undemanding<sup>5</sup> in the Butler PWBA fitting procedure, which employs parameter adjustment. Furthermore, such bland angular distributions have important contributions from low partial waves. In this case the single-channel distorted-wave Born approxi-

mation (DWBA) theory is also somewhat in question.<sup>6,7</sup> As a consequence, it appears that angular distributions are presently incapable of providing an unambiguous test of the " $D$  concept."

In  $(d,p)$  reactions,  $p$ - $\gamma$  correlation measurements offer an alternative and often sensitive means of assessing distortions. A qualitative criterion, that stripping reactions proceeding via capture of a plane-wave particle produce the maximum possible correlation anisotropy,<sup>8</sup> can be applied to infer the presence of distortions without reference to a particular theory of stripping.

In order to systematically test for the dependence of distortions on  $D$ , we have made angular correlation measurements on the reaction  $B^{11}(d,p)B^{12}_{0.95}$ . This reaction is among those which had been inconclusively studied in this context via angular distributions.<sup>3</sup> Only two previous angular correlation measurements have been reported for this reaction.<sup>9,10</sup> They are limited in scope and precision, and are therefore inadequate for illumination of the present problem.

This reaction appears *a priori* as a highly favorable case for study. It has a low  $Q$  value, thus allowing low values of  $D$  to be reached. The low-target  $Z$  should minimize Coulomb distortions. Since this reaction has  $l=1$  angular momentum transfer, the stripping correlation patterns are limited in complexity to order  $P_2$ . Total yield measurements in the region  $E_d=1.0$ – $4.0$  MeV,<sup>3</sup> show a smooth curve indicating the absence of strong compound-nucleus resonances. The proton angular distributions have been measured at 16 different bombarding energies in the range  $E_d=0.7$  to  $8.0$  MeV and in all cases are well fit by Butler theory at forward angles with the angular span of close agreement increasing with decreasing  $E_d$ .<sup>3,9,11–14</sup>

\* Research supported by the National Science Foundation.

† Present address: Center for Naval Analyses, Arlington, Virginia.

<sup>1</sup> D. H. Wilkinson, *Phil. Mag.* **3**, 1185 (1958).

<sup>2</sup> E. K. Warburton and D. W. Chase, Jr., *Phys. Rev.* **120**, 2095 (1960).

<sup>3</sup> J. P. F. Sellschop and D. W. Mingay, in *Proceedings of the Conference on Direct Interactions and Nuclear Reaction Mechanisms*, edited by E. Clementel and C. Villi (Gordon and Breach Science Publishers Inc., New York, 1961), p. 425.

<sup>4</sup> R. D. Amado, *Phys. Rev. Letters* **2**, 399 (1959); I. S. Shapiro, *Nucl. Phys.* **28**, 244 (1961).

<sup>5</sup> See, e.g., N. Austern, in *Proceedings of the Czechoslovakian Summer School* (International Atomic Energy Commission, Vienna, 1963), p. 17.

<sup>6</sup> See, e.g., Roland Omnes, *Phys. Rev.* **137**, B649 (1965).

<sup>7</sup> Howard J. Schnitzer, *Rev. Mod. Phys.* **37**, 666 (1965).

<sup>8</sup> G. R. Satchler, in *Comptes Rendus du Congrès International de Physique Nucléaire, Paris 1958*, edited by P. Gugenberger (Dunod Cie., Paris, 1959), p. 101.

<sup>9</sup> Francis Beck, *Ann. Phys. (Paris)* **1**, 503 (1966).

<sup>10</sup> S. Gorodetzky *et al.*, *J. Phys. Radium* **22**, 575 (1961).

<sup>11</sup> D. Kamke and P. Kramer, *Z. Physik* **168**, 465 (1966).

<sup>12</sup> B. A. Robson and E. Weigold, *Nucl. Phys.* **46**, 321 (1963).

<sup>13</sup> A. Gallmann *et al.*, *Phys. Rev.* **138**, B560 (1965).

<sup>14</sup> J. R. Holt and T. N. Marsham, *Proc. Phys. Soc. (London)* **A66**, 1032 (1953).

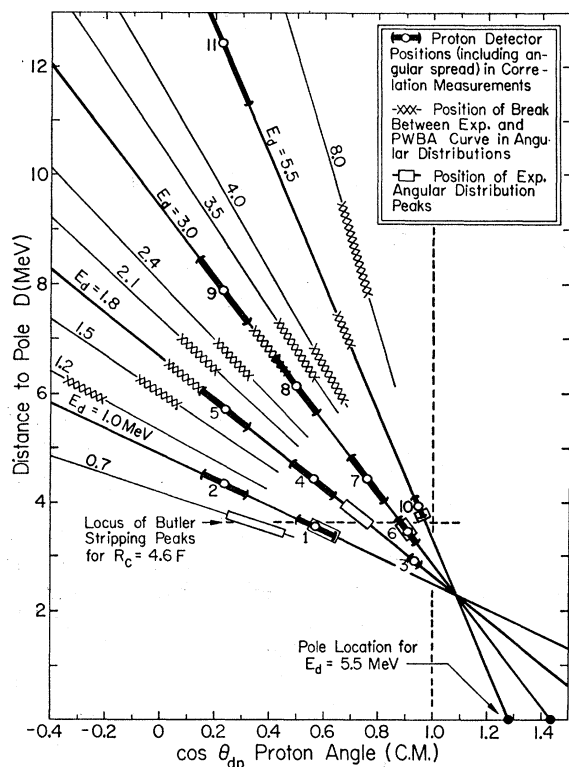


FIG. 1. Distance to the Butler pole versus proton angle for various laboratory deuteron energies,  $E_d$ .

From certain shell-model predictions,<sup>15,16</sup> this reaction would be expected to proceed mainly by  $p_{1/2}$  neutron capture. Since  $p_{1/2}$  capture leads to an isotropic correlation, it would appear that this reaction might be an unfavorable choice for study. However, interference of  $p_{1/2}$  and  $p_{3/2}$  components produces anisotropies considerably larger than our experimental resolution, thus allowing us to measure changes in the anisotropy with sufficient accuracy.

## II. CONSIDERATIONS OF THE $D$ CONCEPT

To display the role of  $D$ , the cross section for a  $(d,p)$  reaction is written:

$$\frac{d\sigma}{d\Omega} \sim \left| \frac{F_1 F_2}{D} + \text{other terms} \right|^2. \quad (1)$$

Here  $F_1$  and  $F_2$  are essentially deuteron and nuclear form factors, and  $D = q^2 + k^2$ , where  $q$  is the momentum transferred to the nucleus and  $k$  is the wave number of the captured neutron. The first term in Eq. (1) is taken to be the amplitude calculated in the Butler stripping theory,<sup>17</sup> and "other terms" account for all possible

interactions not included in the first, e.g., stripping distortions as treated in DWBA.

Dominance by the first term of Eq. (1) for small values of  $D$ , i.e., near enough to the "Butler pole," has been tested<sup>2,3,18,19</sup> in angular distributions by the quality of the fit to PWBA theoretical predictions. In these experiments an approximately constant "break" value of  $D$  was found, independent of  $E_d$  but different for each reaction, below which the distribution shape could be fit by PWBA and above which PWBA failed to fit. As mentioned previously, there has been contention that such a result might be fortuitous.

In terms of common reaction variables, the distance  $D$  to the stripping pole for the reaction  $B^{11}(d,p_1)B^{12*}$ , can be written as

$$D = 3.18E_d + 1.85Q + \epsilon - 2[2E_d(0.92Q + 1.09E_d)]^{1/2} \cos\theta_{dp}, \quad (2)$$

where  $E_d$  is the center-of-mass deuteron energy (i.e.,  $E_d = 0.72E_d$  lab),  $\epsilon (= 2.23$  MeV) is the deuteron binding energy,  $\theta_{dp}$  is the angle between the incident deuteron and outgoing proton directions in the c.m. system, and  $Q = 0.19$  MeV. Equation (2) was derived without invoking the infinite-target-mass assumption<sup>2</sup> and therefore leads to slightly different values from those in Ref. 3.

A plot of  $D$  versus  $\cos\theta_{dp}$  as given in Fig. 1 provides a convenient format for displaying the systematics of

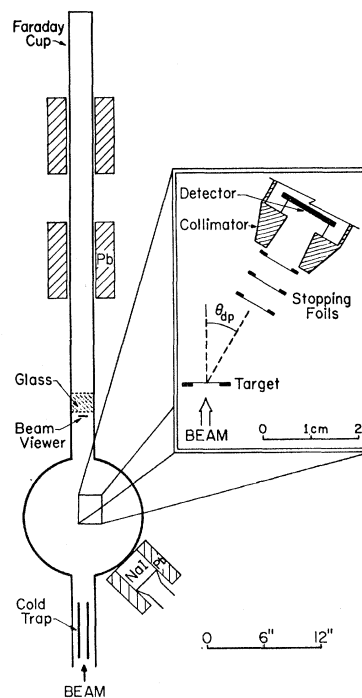


FIG. 2. Typical scattering chamber and detector arrangement, viewed from above.

<sup>15</sup> D. Kurath, Phys. Rev. **101**, 216 (1956).  
<sup>16</sup> D. Amit and A. Katz, Nucl. Phys. **58**, 388 (1964).  
<sup>17</sup> S. T. Butler and O. H. Hitmair, *Nuclear Stripping Reactions* (Horwitz Publications, Inc., Sydney, 1957); M. H. Macfarlane and J. B. French, Rev. Mod. Phys. **32**, 567 (1960).

<sup>18</sup> W. Schier *et al.*, Nucl. Phys. **88**, 373 (1966).  
<sup>19</sup> R. V. Poore, P. E. Shearin, D. R. Tilley, and R. M. Williamson, Nucl. Phys. **A92**, 97 (1967).

interest. Lines of constant  $E_d$  (lab values are shown) have negative slope and intercept  $D=0$  (the pole) at unphysical values of  $\cos\theta_{dp}$ . Increasing  $E_d$  leads to decreasing  $\cos\theta_{dp}|_{\text{pole}}$  (i.e.,  $\cos\theta_{dp}$  at  $D=0$ ) and vice versa. Several authors<sup>4,20</sup> have emphasized the need to reduce  $\cos\theta_{dp}|_{\text{pole}}$  in order to get close to the pole. From Fig. 1 it is clear that small  $D$  values over an appreciable range of angles are attained at a cost of increasing  $\cos\theta_{dp}|_{\text{pole}}$ .

The "break  $D$ " values observed by Sellschop<sup>3</sup> are pictured in Fig. 1. Inclusion of "break  $D$ " locations from angular distribution measurements at  $E_d=5.5$  and 8.0 MeV<sup>13,14</sup> indicates that the approximate constancy of this quantity is violated as higher deuteron energies are reached.

We have noted that the experimental stripping peak locations can also be characterized by a constant  $D$  value (see Fig. 1). This is not unexpected since Butler theory gives peak locations for the condition  $\mathbf{l} = \mathbf{R}_c \times \mathbf{q}$ . Constant cutoff radius  $R_c$  therefore implies constant  $q$  and hence constant  $D$ , in a given reaction. Increasing  $R_c$  leads to lower  $D$  values for the peak locations and

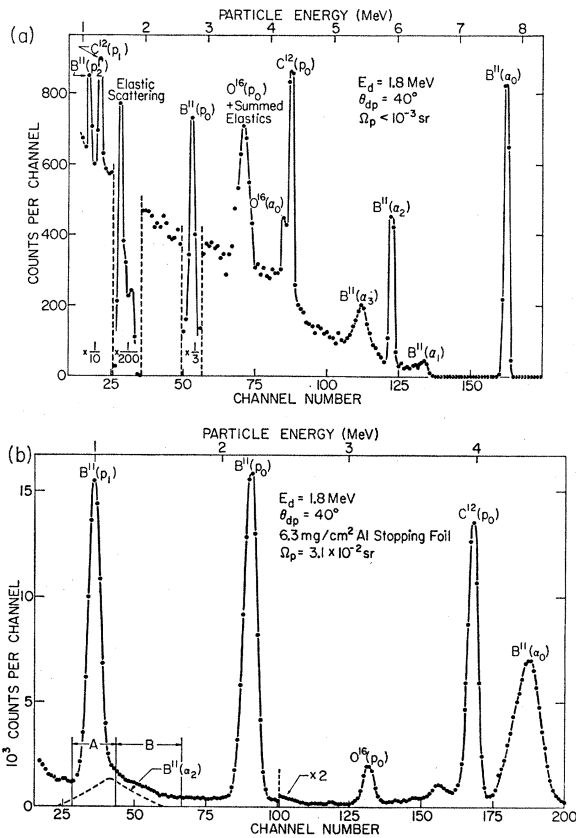


FIG. 3. Pulse-height spectra from solid-state proton detector. (a) Spectrum without stopping foils. (b) Spectrum with 6.3-mg/cm<sup>2</sup> aluminum stopping foil. (In a comparison of these spectra, a change in detector solid angle and in target impurity concentration is to be noted.)

<sup>20</sup> H. J. Schnitzer, Nucl. Phys. 36, 505 (1962).

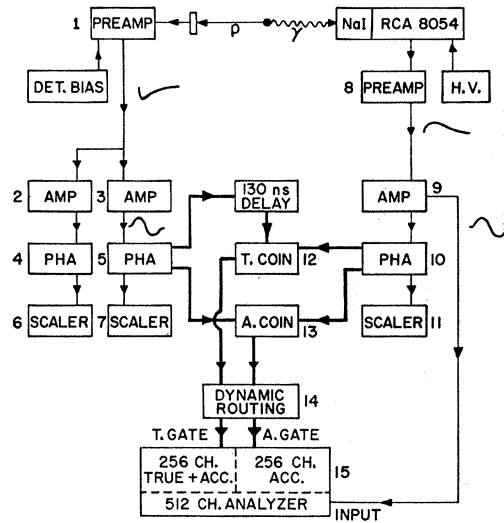


FIG. 4. Block diagram of electronic equipment for  $p$ - $\gamma$  correlation measurements.

vice versa. It is interesting to note from Fig. 1 that  $R_c$  is ultimately forced to smaller values by increasing  $E_d$  (i.e., "peak  $D$ " must remain in the physical region). Conversely, as  $E_d$  is decreased, the peak will move to back angles if constant  $R_c$  is maintained.

In this experiment, eleven reaction-plane angular correlations were measured over the deuteron energy range 1.0–5.5 MeV. The energy-proton angle locations for each measurement are shown and numbered in Fig. 1. The basic objective of these measurements was to see if the correlation parameter systematically tended toward PWBA predictions as  $D$  was lowered, independent of what energy-angle choices were exercised in achieving a given  $D$  value. In addition to this objective, several other experimental tests are implied by the choice of energy-proton angles. Measurements 2, 5, 9, and 11 study the effect of moving the pole location with  $\cos\theta_{dp}$  fixed. Measurements 2, 4, and 7 study constant  $D$  under the influence of variable  $E_d$  and  $\theta_{dp}$ . Points 1, 6, and 10 do the same with constant  $D$  being on the stripping peaks. Finally, 3 represents the lowest  $D$  value attained.

In contrast to the above classifications, it is to be noted that point 10 represents the most favorable condition for stripping based on the usual PWBA criteria.<sup>17</sup> This point is on the stripping peak at the highest deuteron energy used in this experiment.

### III. EXPERIMENTAL TECHNIQUE

Deuterons from the University of Virginia 5.5-MeV Van de Graaff were used to bombard thin (20–40  $\mu\text{g}/\text{cm}^2$ ) targets of isotopically enriched (98%) boron-11.<sup>21</sup> The target films, prepared by electron beam evaporation, were mounted either self-supporting or on very thin (5–10  $\mu\text{g}/\text{cm}^2$ ) backings of Formvar or carbon.

<sup>21</sup> A. Borden, Ph.D. thesis, University of Virginia, 1966 (unpublished).

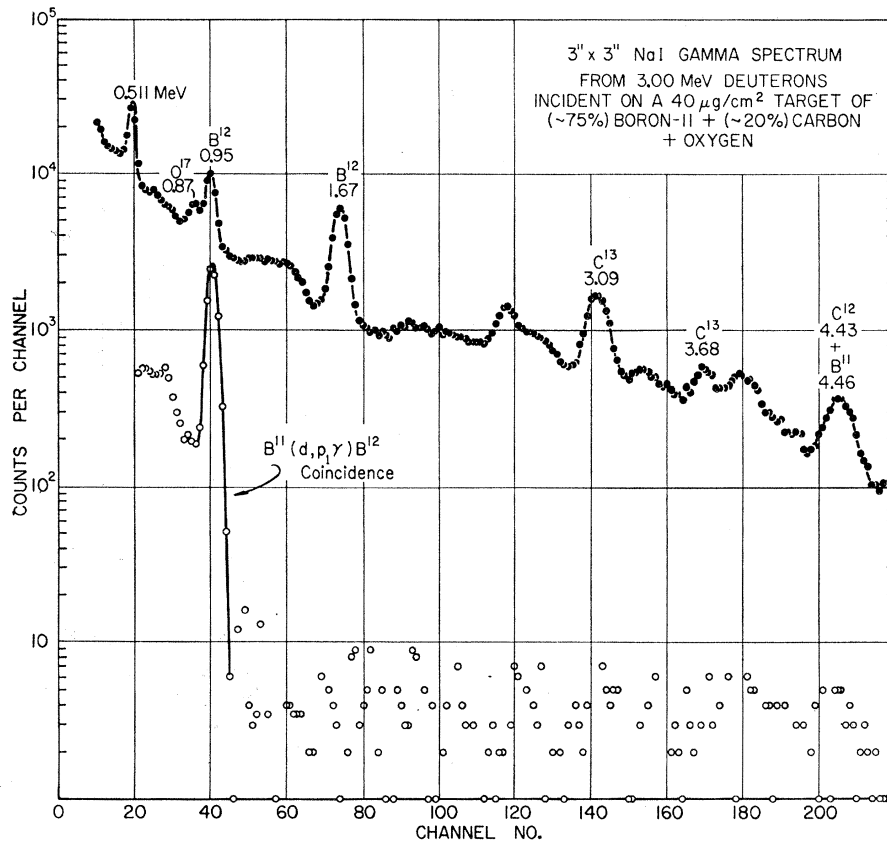


FIG. 5. Scintillation pulse-height spectra produced by bombardment of a  $B^{11}$  target with deuterons. Solid dots—singles spectrum. Open circles—spectrum in coincidence with protons corresponding to  $B^{12}$  left in first excited state.

The target and proton detector were located in a 12-in.-diam stainless steel scattering chamber with 0.400-in. walls (Fig. 2). For a given correlation measurement, the vertical positioning of the target was held fixed but small rotations about the vertical were employed to avoid shadowing the gamma detector with the target mount. Carbon deposition onto the target was measured to be about  $1 \mu\text{g}/\text{cm}^2$  over a complete correlation run. The beam spot size was usually 1–2-mm diam and the current was typically  $0.1 \mu\text{A}$ .

The gamma detector, a 3-in.  $\times$  3-in. NaI scintillator mounted on an RCA 8054 photomultiplier, was positioned external to the chamber as pictured in Fig. 2. With the proton detector held fixed, the  $p$ - $\gamma$  correlation was measured by observing the 0.95-MeV photopeak coincidence yield in the horizontal or reaction plane, for various positions of the gamma detector. By measuring the yield versus angle of the 1.06-MeV gamma radiation from a 2-mm-diam disk-shaped  $Bi^{207}$  source placed at the beam-on-target-spot, small variations (1–2%) in the detector solid angle and in the chamber wall transmission properties were mapped for use in the normalization of  $p$ - $\gamma$  yields.

An ORTEC silicon surface barrier detector, usually biased to a depletion depth of about  $260 \mu$ , was used for proton detection. Because the protons of interest had energies comparable to those of the elastically scattered deuterons, it was necessary to employ aluminum stop-

ping foils to remove the bulk of the elastically scattered particles. With the appropriate thickness of foils in use, the  $B^{11}(d, p_1)B^{12*}$  proton group formed a clearly resolved (in energy) peak, which was singled out for coincidence analysis by means of a single channel analyzer. Figure 3 shows typical spectra of the proton detector, with and without stopping foils.

A schematic diagram of the electronic setup is shown in Fig. 4. Commercial electronic modules comprised all but the routing circuitry. Two matched-width ( $2\tau \approx 60$  nsec) fast coincidence circuits along with a dynamic routing system were used to provide on-line evaluation of the accidental coincidence spectrum. The photopeak counting rate for true events typically was about 30 counts per min and the true-to-accidental counting ratio, averaged under this peak, was typically about 20 to 1. Singles and coincidence-gated gamma spectra as observed at  $E_d = 3.0$  MeV are shown in Fig. 5. The coincidence spectrum shown is for true counts only, i.e., accidental events have been subtracted out.

A small percentage ( $\sim 1$ –4%) of true coincidence counts from sources other than  $B^{11}(d, p_1\gamma)B^{12*}$  was always "observed" under the gated 0.95-MeV photopeak. The accurate subtraction of these counts from the counts of interest was accomplished via an analysis<sup>21</sup> of the true counts above the peak where a fairly smooth spectrum was usually observed. These counts are thought to correspond to  $p$ - $\gamma$  and  $\beta$ - $\gamma$  coincidences

arising principally from three processes:  $B^{10}(d,p)B^{11*}_{8.95}(\gamma)B^{11}$ ,  $B^{12}(\beta^-)C^{12*}(\gamma)C^{12}$ , and  $B^{12}(\beta^-)$  bremsstrahlung. The background contribution from these sources was evaluated by extrapolating the average level of counts above the peak back into the 0.95-MeV region. At the lower deuteron energies (1.0 and 1.8 MeV), alpha-neutron coincidences from many-body ( $3\alpha+n$ ) final states produced<sup>22</sup> by  $B^{11}(d,n)$  and  $B^{11}(d,\alpha)$ , were present as an additional background source. Subsidiary experiments showed that  $\alpha$ - $n$  background contributions were of the order of several percent and had a tendency to peak around  $E=0.85$  MeV, probably indicating the presence of the  $Fe^{56}(n,n'\gamma)Fe^{56}$  reaction<sup>23</sup> in the chamber walls. Detailed analysis<sup>21</sup> of individual spectra from the correlation measurements, particularly in the  $E_\gamma=0.85$ -MeV region, showed that  $\alpha$ - $n$  contributions typically did not exhibit strong angular dependence. In general, the evaluation and subtraction of the total true background was accomplished with an estimated probable error of 0.7% relative and 1.0% absolute on each point. A summary of estimated experimental error is given in Table I.

Three independent measurements of the relative beam flux or reaction rate were employed to insure accurate normalization of each  $p$ - $\gamma$  yield within a given correlation measurement. These were: (1) standard integration of the beam current via a Faraday cup, (2) a monitor of the protons from  $B^{11}(d,p_1)B^{12*}$ , and (3) a monitor of the alphas from boron ( $d,\alpha$ ). For monitor (3), the strong, well-isolated  $B^{11}(d,\alpha_0)Be^9$  reaction peak was monitored at the lower deuteron energies. At  $E_d=3.0$  MeV, the increased stopping foil thickness shifted this peak into more cluttered regions of the spectrum and it was necessary to turn to the

TABLE I. Summary of experimental error on a given point within a correlation set; estimated probable values are listed.

Source	Relative error (%)	Absolute error (%)
Counting statistics (typical $\sigma=4.0\%$ )	$\sigma$	$\sigma$
Gamma detector geometry	0.6	0.6
Identification of photopeak counts	1.0	1.0
Subtraction of accidental counts	0.3	0.7
Beam flux normalization (typical)	0.8	0.8
Subtraction of true background (typical)	0.7	1.0
Variation in accidental summing losses	0.4	0.4
Sum	$(\sqrt{2.7+\sigma^2})$	$(\sqrt{3.4+\sigma^2})$

weaker  $B^{10}(d,\alpha_0)Be^8$  and  $B^{10}(d,\alpha_1)Be^{8*}$  alpha peaks. Finally at  $E_d=5.5$  MeV no suitable peaks were available for this particular monitor. The relative consistency of these three (or two) measurements was used to establish an estimate of the probable error in beam flux normalization. This error was about 1% in the worst cases.

#### IV. CORRELATION DATA

The correlation data were analyzed on the University of Virginia Burroughs B5500 computer using a special nonlinear least-squares fitting program developed here.<sup>24</sup> This data, along with the best-fitting three-parameter curve normalized to the form

$$W(\phi_\gamma) = 1 - \epsilon \cos 2(\phi_\gamma - \phi_0), \quad (3)$$

are presented in Figs. 6-9. Error bars on the data points in these figures correspond to  $\sigma$  (Table I). The extracted parameters and their corresponding uncertainties are summarized in Table II. Anisotropy values  $\epsilon$  are listed without correction for attenuation due to the finite angular resolution.<sup>25</sup> Neglecting very small

TABLE II. Angular correlation parameters from computed best fits to experimental data. Quantities given in parentheses are from analysis where the worst outlying point has been omitted in each set of data. Column designations: (A) Correlation number. (B) Incident lab deuteron energy. (Best estimates:  $1.010 \pm 0.003$ ,  $1.801 \pm 0.003$ ,  $2.975 \pm 0.003$ ,  $5.48 \pm 0.02$  MeV. Typical half-thickness of target was 3 keV.) (C) Distance to pole. (D) Proton angle in the c.m. system. (E) and (F) See Fig. 6. (G) Anisotropy from best fit of Eq. (3). (H) Anisotropy from best fit of  $W(\phi_\gamma) = 1 - \epsilon' P_2[\cos(\phi_\gamma - \phi_0)]$ .

(A)	(B) $E_d$ (MeV)	(C) $D$ (MeV)	(D) $\theta_{dp}$ (deg)	(E) $\Phi_r$ (deg)	(F) $\Phi_0$ (deg)	(G) $\epsilon$ (%)	(H) $\epsilon'$ (%)
1	1.0	3.5	54.9	47.2	44.7 ± 7.0 (46.4 ± 6.5)	8.5 ± 1.1 (9.2 ± 1.2)	11.6 ± 1.6
2	1.0	4.3	76.0	41.7	35.9 ± 8.3	8.4 ± 1.7	11.5 ± 2.4
3	1.8	2.9	19.5	36.5	40.4 ± 10.0 (42.3 ± 9)	6.1 ± 1.2 (6.9 ± 1.2)	8.3 ± 1.6
4	1.8	4.4	55.1	45.0	71.0 ± 4.8	7.7 ± 1.6	10.5 ± 2.2
5	1.8	5.7	76.3	40.1	96.2 ± 4.5	8.8 ± 2.4	12.1 ± 3.4
6	3.0	3.4	24.5	39	36.4 ± 5.8	7.9 ± 0.9	10.8 ± 1.3
7	3.0	4.4	40	44.2	48.4 ± 6.2 (49.6 ± 5.8)	6.4 ± 0.8 (6.8 ± 0.8)	8.8 ± 1.1
8	3.0	6.1	60.6	40.0	74.9 ± 6.3	9.3 ± 2.4	12.8 ± 3.4
9	3.0	7.9	76.4	39.2	95.0 ± 6.8	5.5 ± 2.6	7.5 ± 3.6
10	5.5	3.9	19	33	40.4 ± 5.2 (42.2 ± 5.5)	11.3 ± 1.0 (10.7 ± 1.0)	15.7 ± 1.5
11	5.5	12.3	76.6	38.7	176.9 ± 6.1	5.7 ± 2.3	7.8 ± 3.2

<sup>22</sup> F. Ajzenberg-Selove and T. Lauritsen, Nucl. Phys. **11**, 1 (1959).

<sup>23</sup> R. W. Benjamin *et al.*, Nucl. Phys. **79**, 241 (1966).

<sup>24</sup> G. Hancock (private communication).

<sup>25</sup> M. E. Rose, Phys. Rev. **91**, 610 (1953).

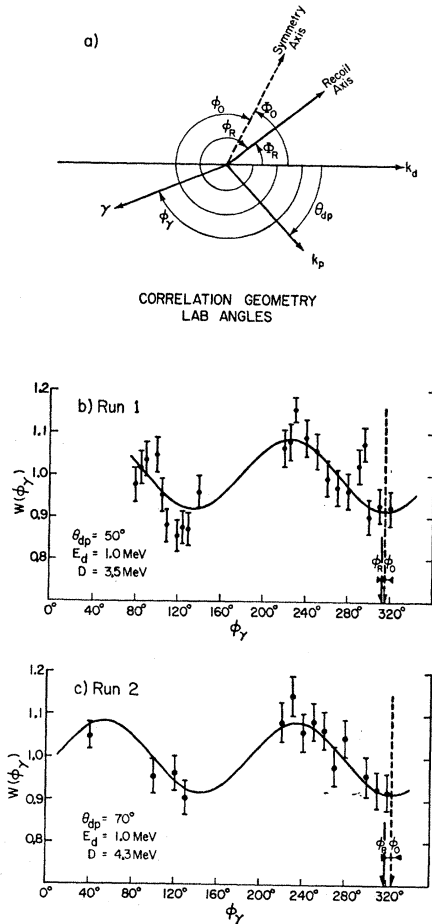


FIG. 6. (a) Correlation geometry, defining the angles used here. (b)  $p$ - $\gamma$  correlation for run No. 1; solid line  $W = 1 - 0.085 \cos^2 \times (\phi_\gamma - 45^\circ)$ . (c)  $p$ - $\gamma$  correlation for run No. 2; solid line  $W = 1 - 0.084 \cos^2(\phi_\gamma - 36^\circ)$ .

smearing effects introduced by Compton scattering in the chamber wall, the multiplicative correction factor is  $1.037 \pm 0.006$ , based in part on an interpolation of  $J_2/J_0$  values measured by Herskind<sup>26</sup> for photopeak counting.

TABLE III. Goodness-of-fit probability from  $\chi^2$  test.

Correlation number	1-parameter fit	3-parameter fit	3-parameter fit without outlying point	5-parameter fit
1	$\ll 0.001$	0.02	0.3	0.02
2	$\ll 0.001$	0.8		0.7
3	$\ll 0.001$	0.05	0.4	0.05
4	$\ll 0.001$	0.6		0.6
5	0.02	0.6		0.8
6	$\ll 0.001$	0.6		0.5
7	$\ll 0.001$	0.01	0.04	0.01
8	0.03	0.5		0.5
9	0.8	0.9		0.8
10	$\ll 0.001$	0.02	0.2	0.01
11	0.4	0.7		0.8

<sup>26</sup>B. Herskind and Y. Yoshizawa, Nucl. Instr. Methods 27, 104 (1964).

In addition to finding the best three-parameter fit, the computer program calculated one- and five-parameter fits (i.e., including  $\cos 4\phi_\gamma$  terms) and their corresponding goodness-of-fit probability  $P$  from  $\chi^2$  tests. The resulting  $P$  values, summarized in Table III, show that a three-parameter fit is as good as, or better than, other fits in all cases. In four of the eleven correlations,  $P$  fell outside the usual acceptability range of  $0.9 > P > 0.1$ . Inspection of the data showed that these four cases each had a possible "outlying" data point lying more than  $2.5\sigma$  away from the best-fitting three-parameter curve, whereas none of the other seven correlations had points that far off. Reanalysis of these four cases, with the "outlying" point omitted in each set, showed that three of the four cases had acceptable  $P$  values and that the correlation parameters were only slightly changed, as indicated in Table II. Parameters from analysis where the "outlying" point was included were taken as the accepted values for comparison to theory.

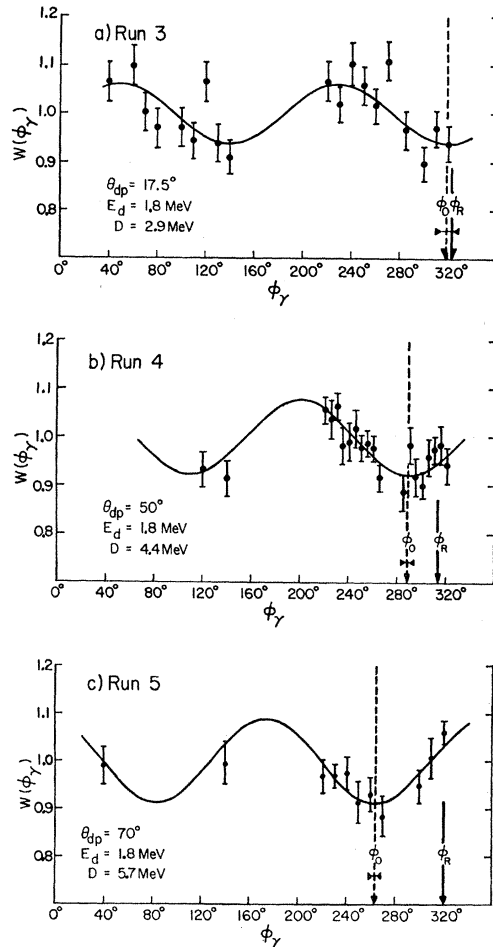


FIG. 7. (a)  $p$ - $\gamma$  correlation for run No. 3; solid line  $W = 1 - 0.061 \times \cos^2(\phi_\gamma - 40^\circ)$ . (b)  $p$ - $\gamma$  correlation for run No. 4; solid line  $W = 1 - 0.077 \cos^2(\phi_\gamma - 71^\circ)$ . (c)  $p$ - $\gamma$  correlation for run No. 5; solid line  $W = 1 - 0.088 \cos^2(\phi_\gamma - 96^\circ)$ .

## V. DISCUSSION

## A. Relevant Angular Correlation Theory

In the case of  $l=1$  stripping, the experimental parameters extracted for comparison with theory are the correlation anisotropy  $\epsilon$  and the correlation symmetry axis  $\phi_0$ . PWBA theory predicts that the laboratory recoil axis is the symmetry axis for the correlation pattern and that the correlation anisotropy is constant, independent of  $E_d$  and  $\theta_{dp}$ . Considerations on distortions, and in particular DWBA theory,<sup>27</sup> predict that  $\phi_0$  is in general shifted away from the recoil direction and that  $\epsilon$  is reduced from the PWBA value.

For convenience, we will discuss our results in the framework of a frequently used form of DWBA theory,<sup>27</sup> but with slight modifications. Equation (3) introduces a negative sign which is not conventional, and it also

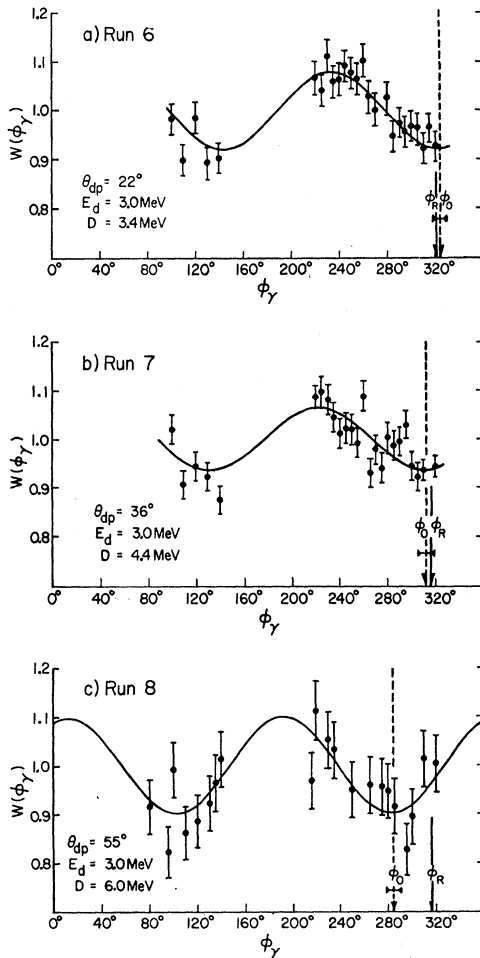


FIG. 8. (a)  $p$ - $\gamma$  correlation from run No. 6; solid line  $W=1-0.079 \cos 2(\phi_\gamma-36^\circ)$ . (b)  $p$ - $\gamma$  correlation for run No. 7; solid line  $W=1-0.064 \cos 2(\phi_\gamma-48^\circ)$ . (c)  $p$ - $\gamma$  correlation for run No. 8; solid line  $W=1-0.093 \cos 2(\phi_\gamma-75^\circ)$ .

<sup>27</sup> G. R. Satchler and W. Tobocman, Phys. Rev. **118**, 1566 (1960); R. Huby, M. Y. Refai, and G. R. Satchler, Nucl. Phys. **9**, 94 (1958).

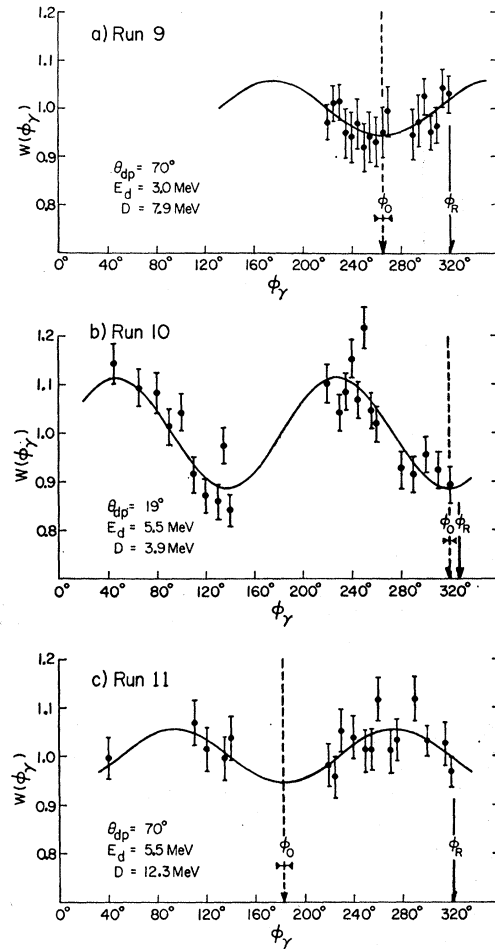


FIG. 9. (a)  $p$ - $\gamma$  correlation for run No. 9; solid line  $W=1-0.055 \cos 2(\phi_\gamma-95^\circ)$ . (b)  $p$ - $\gamma$  correlation for run No. 10; solid line  $W=1-0.113 \cos 2(\phi_\gamma-40^\circ)$ . (c)  $p$ - $\gamma$  correlation for run No. 11; solid line  $W=1-0.057 \cos 2(\phi_\gamma+3^\circ)$ .

implies an altered, but useful magnitude for  $\epsilon$ . Our results, then, should be compared with a theoretical equation, in the notation of Ref. 7,

$$\epsilon = \frac{-3g_2\lambda}{4+g_2} \quad (4)$$

Here  $\lambda$  is a distortion-dependent parameter,  $0 \leq \lambda \leq 1$ , which in PWBA theory takes the value unity. Thus  $\epsilon_{\text{DWBA}} = \lambda \epsilon_{\text{PWBA}}$ . The theoretical form<sup>27,28</sup> for  $g_2$  in the present correlation is

$$g_2 = [\theta_{3/2}^2 \eta_2 (\frac{3}{2} \frac{3}{2} \frac{3}{2} J_e) + 2\theta_{1/2} \theta_{3/2} \eta_2 (\frac{1}{2} \frac{3}{2} \frac{3}{2} J_e)] \\ \times [C_1^2 F_2(11J_e) + (2\sqrt{75}) C_1 C_2 G_2(121J_e) \\ + C_2^2 F_2(21J_e)] \quad (5) \\ = \frac{1}{(1+x^2)(1+\delta^2)} [\eta_2 (\frac{3}{2} \frac{3}{2} \frac{3}{2} J_e) + 2x\eta_2 (\frac{1}{2} \frac{3}{2} \frac{3}{2} J_e)] \\ \times [F_2(11J_e) + 2(\sqrt{75})\delta G_2(121J_e) + \delta^2 F_2(21J_e)].$$

<sup>28</sup> G. R. Satchler, Proc. Phys. Soc. (London) **A66**, 1081 (1953).

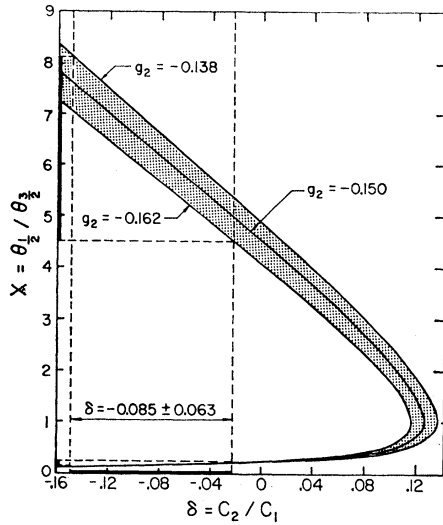


FIG. 10. Plot of transferred neutron spin mixing parameter  $x$  versus gamma decay multipolarity mixing parameter  $\delta$ , as limited by present correlation measurements for the  $B^{11}(d, p\gamma)B^{12*}_{0.95}$  reaction. As explained in the text, theoretical considerations much favor the upper branch. Limitations on  $\delta$  as pictured are from Ref. 9.

The functions  $\eta_2$  are tabulated in Ref. 28 and the functions  $F_2$  and  $G_2$  are tabulated in Ref. 29;  $\theta_{3/2}$  and  $\theta_{1/2}$  are the normalized reduced width amplitudes for the two possible  $j$  states for the captured neutron if  $l_n=1$ ;  $C_1$  and  $C_2$  are the normalized reduced matrix elements for  $M1$  and  $E2$  gamma transitions to the final state;  $x \equiv \theta_{1/2}/\theta_{3/2}$ ;  $\delta \equiv C_2/C_1$ ; and  $J_e$  is the spin of the first excited state of  $B^{12}$ .

We apply this theory in two ways: in the spectroscopic analysis and, less quantitatively, in the reaction mechanism discussion.

### B. Spectroscopic Analysis

We have not measured  $\lambda$  directly in this experiment, but it is useful to proceed on the assumption (One cannot theoretically preclude the possibility of observing anisotropies larger than the PWBA limit since the effects of compound nucleus formation as a competing reaction mode are unknown. We assume domination by the stripping mode, citing the following items as support for this assumption: The proton angular distribution in this case shows a well-developed stripping pattern. The proton detector was positioned on the stripping peak in order to diminish relative contributions from the compound nucleus mode, if present. The observed correlation pattern was oriented approximately along the direction expected for a PWBA stripping process and it was of complexity  $P_2$ , consistent with an  $l=1$  neutron capture) that the PWBA limit,  $\lambda=1$ , is closely approximated in correlation No. 10 where the largest value of

$\epsilon$ ,  $0.113 \pm 0.01$ , is observed. This assumption is supported by specific DWBA calculations presented in Sec. V C.

After correction for finite angular resolution, the PWBA anisotropy is  $\epsilon = 0.117 \pm 0.01$ . From Eq. (4) this implies  $g_2 = -(0.150 \pm 0.012)$ , the value which we will use in this analysis.

The use of the value of  $g_2$  in determining  $x$  from Eq. (5) depends on a knowledge of  $J_e$  and  $\delta$ . The value  $2^+$  had been assigned<sup>30</sup> to the state  $J_e$  based on a measurement<sup>10</sup>  $\epsilon = -0.24 \pm 0.05$  (in our notation). This disagrees both in sign and magnitude with the present result. Taking our sign determination, a spin assignment of  $1^+$  is not eliminated by present available data.<sup>31</sup>

On theoretical grounds the assignment of  $2^+$  as the spin parity of the first excited state of  $B^{12}$  is nearly unassailable. This state seems to be established as the analog of the  $2^+T=1$  state at 16.11 MeV in  $C^{12}$  (see e.g., Ref. 13). Moreover, the likelihood for the alternative, that is the existence of another  $1^+$  state within 5 MeV of the  $1^+$  ground state of  $B^{12}$  seems small; a major shell-breaking would be required for such a state. We will therefore, proceed on the assumption that  $J_e = 2^+$ . In this case Eq. (5) becomes:

$$g_2 = \frac{-x}{(1+x^2)(1+\delta^2)} (0.700 - 0.500\delta^2 - 3.13\delta). \quad (6)$$

Assuming  $J_e = 2^+$  and  $g_2 = -0.150 \pm 0.012$ , we find by Eq. (6) that  $x$  is positive and restricted in magnitude as pictured in Fig. 10. The restriction shown on  $\delta$ , i.e.,  $\delta = -0.085 \pm 0.063$ , is from the Strasbourg results,<sup>9</sup> based on gamma-ray angular distribution and polarization measurements at 0.7-MeV bombarding energy. An alternative value for  $\delta \gg 1$  permitted by that experiment would be inconsistent with the measured lifetime of the state ( $\tau = (3.4 \pm 1) \times 10^{-13}$  sec).<sup>30</sup> If our value for  $g_2$  is low (i.e., if the case  $\epsilon = 0.117$  in fact corresponds to some  $\lambda < 1$ ) the  $x$  values consistent with the correct  $g_2$  would be further restricted as can be seen from Fig. 10.

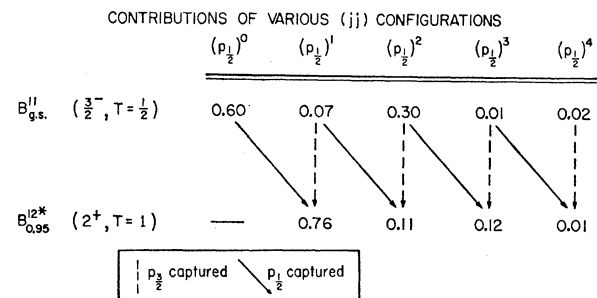


FIG. 11. Components of shell model  $(jj)$  configurations in the  $B^{11}_{g.s.}$  and  $B^{12*}_{0.95}$  states, and the effect of adding  $p$ -wave neutrons.

<sup>29</sup> L. C. Biedenharn and M. E. Rose, Rev. Mod. Phys. **25**, 729 (1953).

<sup>30</sup> E. K. Warburton and L. F. Chase, Jr., Phys. Rev. **132**, 2273 (1963).

<sup>31</sup> E. K. Warburton (private communication).



On a theoretical basis, we can limit the value of  $x$  further. With the assumption that the 0.95-MeV state is  $2^+$ , experimenters have determined<sup>13,14,17</sup> its spectroscopic factor in  $B^{11}(d,p)B^{12}_{0.95}$  to be  $\sim 0.6$  to  $0.7$ . Consequently the state must have a wave function which has a good overlap with that of the ground state of  $B^{11}$  plus a  $1p$  neutron. Shell-model theory<sup>15,16</sup> has predicted that the  $\frac{3}{2}^-$  ground state of  $B^{11}$  is largely  $s^4p_{3/2}^7$  and the lowest  $2^+T=1$  state of the 12 nucleon system is largely  $s^4p_{3/2}^7p_{1/2}^1$ . Taken with the large spectroscopic factor, these calculations imply that the transferred neutron in this reaction should be mainly  $p_{1/2}$ . Therefore, the value of  $x^2$  (and thus  $x$ ) should be greater than unity and the upper branch of the curve in Fig. 10 should be the appropriate one.

Figure 11 is a chart which summarizes this situation. It depicts changes in components of the shell model states in this reaction, based on calculations of Ref. 16.

### C. Discussion of Reaction Distortions

It has been emphasized<sup>32</sup> that it does not make sense to ignore distortion completely in any experimentally realizable circumstance. Rigorous application of the  $D$  concept, that is completely ignoring all but the first term of Eq. (1), amounts to just that. A more moderate goal of the concept is to establish criteria under which the distortions could be predicted to be small. In the present work, we have attempted to test for approximate, rather than absolute, validity of the  $D$  concept under conditions (i.e., low  $Q$  and  $E_d$ ) deemed favorable by existing criteria.

If the  $D$  concept were upheld by our data, we would expect our correlation parameters to systematically approach PWBA predictions with decreasing  $D$ . Angular distribution studies<sup>3</sup> indicate that the region  $D=6$  to  $7$  MeV might be a transition region in this respect. We might therefore expect the anisotropy to have a large,

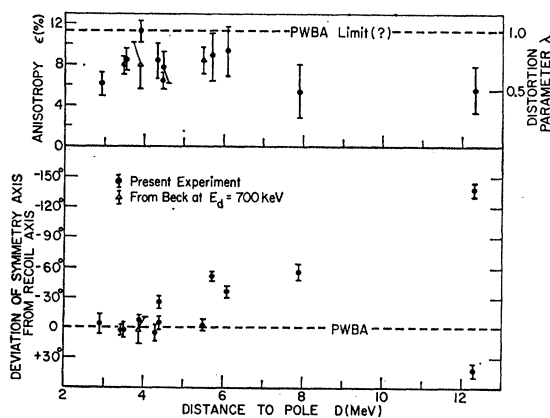


FIG. 12. Measured correlation anisotropy and symmetry axis shift versus distance to the Butler pole.

<sup>32</sup> See, e.g., G. R. Satchler, in *Lectures in Theoretical Physics*, edited by P. D. Kunz, D. A. Lind, and W. E. Brittin, Vol. 8C (University of Colorado Press, Boulder, 1966), pp. 73-175.

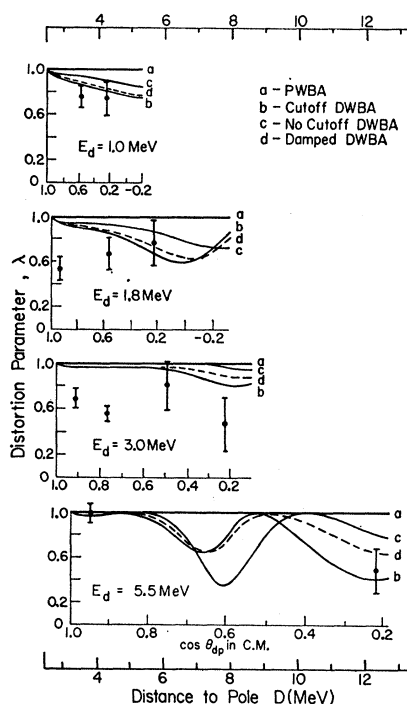


FIG. 13. Distortion parameter  $\lambda$  versus distance to the Butler pole. Experimental values and various theoretical curves are shown for the deuteron energies used in the present experiment.

nearly constant value for  $D \leq 6$  MeV and then typically to take on smaller values for  $D > 6$  MeV. The symmetry axis shift would be essentially zero for  $D \leq 6$  MeV. For  $D > 6$  MeV there might or might not be some symmetry axis shift. The reason for this is that distortions of the incoming and outgoing waves can have opposite contributions to such shifts,<sup>33</sup> resulting in partial or total cancellation. Accompanying cancellation effects do not apply in this way to  $\epsilon$ .

The combined data exhibiting the behavior of the measured correlation parameters is shown in Fig. 12. It is seen that the symmetry axis shifts follow the predicted trend up to  $D \approx 4.5$  MeV. As just explained, this is a necessary but not sufficient condition for PWBA to be dominant below  $D = 4.5$  MeV. However, this is considered to be good evidence<sup>8</sup> for the direct interaction character of the reaction.

In this reaction the momentum conditions for cancelling distortion effects<sup>33</sup> are most nearly met at the lowest deuteron energies which we used, and these generally correspond to lower  $D$  values. We therefore must rely on the anisotropy trends to assess distortions.

As Fig. 12 shows, the above predictions of the  $D$  concept are not borne out in the anisotropy measurements. The largest anisotropy is not found at the smallest value of  $D$ . As a consequence there is no way that this data implies an absence of distortions at low  $D$ . One would like to be able to make the additional

<sup>33</sup> G. R. Satchler, *Nucl. Phys.* **18**, 110 (1960).

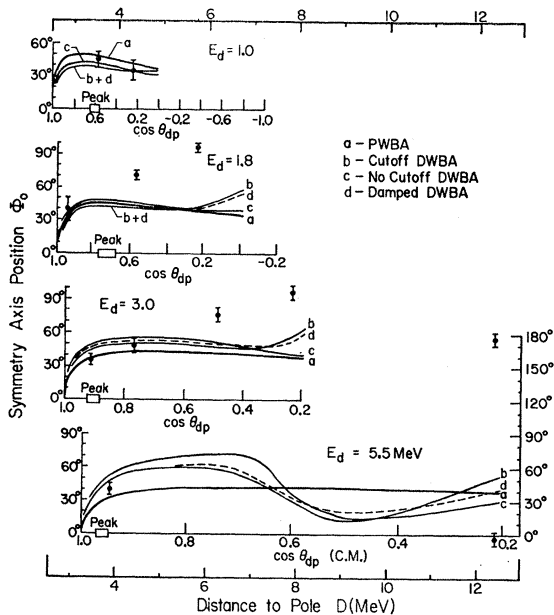


FIG. 14. Symmetry axis  $\Phi_0$  versus distance to the Butler pole. Experimental values and various theoretical curves are shown for the deuteron energies used in the present experiment.

statement that variations in strength of the distortion terms are indicated by the relative values  $\epsilon$  takes on. Such analysis is, however, too simplistic if the nuclear and Coulomb distortions cancel in an irregular manner or if other types of irregular interference phenomena are present. Cancellations of this first type have been discussed with respect to angular distributions.<sup>34</sup>

In order to improve on this qualitative statement about distortions, it is possible to calculate detailed predictions of the correlation parameters by DWBA theory, in which optical model potentials generate the distorted waves. An exemplary calculation of this type has been done for us by G. R. Satchler, using code SALLY.<sup>35</sup> The deuteron optical potential used was from  $C^{12}+d$ , and the proton potential was typical of those discussed by Perey.<sup>36</sup> As only general features of these calculations are examined here, we will not list details of the optical potentials, and we will ignore the possible shortcomings of applying these results to such a light nucleus.

Figures 13 and 14 show the results of the DWBA calculations for three different treatments of the internal nuclear radial wave function, along with PWBA curves and the experimental points. The measured anisotropies have been transferred to the  $\lambda$  scale under the previously employed assumption that  $\lambda=1$  for  $\epsilon=0.113$ .

<sup>34</sup> W. Tobocman, Phys. Rev. **115**, 98 (1959).

<sup>35</sup> R. H. Bassel, R. M. Drisko, and G. R. Satchler, Oak Ridge National Laboratory Report No. ORNL-3240 (unpublished).

<sup>36</sup> F. Perey and B. Buck, Nucl. Phys. **32**, 353 (1962).

With the data plotted in this way, we see that the greatest departure of the experimental values of  $\lambda$  from PWBA predictions are at the intermediate value of energy, 3 MeV. Such a behavior is not predicted by the DWBA curves. In general these DWBA curves closely parallel the PWBA predictions in regions where our data was taken (except for  $\phi_0$ ), and they are therefore inadequate in accounting for the experimental data.

It seems particularly significant that the highest value of  $\lambda$  occurred in our data at the highest bombarding energy, 5.5 MeV, and on the stripping peak. This agreement with traditional stripping expectations<sup>17</sup> is in direct opposition to predictions of the  $D$  concept.

We are aware of two possible explanations for the behavior of our data:

- (1) The "other terms" in Eq. (1) are not becoming unimportant as conditions are changed to reduce  $D$ .
- (2) The PWBA term is not capable of taking on the predicted properties.

With regard to the first point above, our knowledge of the terms of the expansion underlying Eq. (1) is very incomplete.<sup>7</sup> We have calculated the values of  $\cos\theta$  at the simpler singularities given in Ref. 7. They all (except the Coulomb branch point) fall far away from the Butler pole in terms of  $\cos\theta$ . This is considered to be evidence that they are unimportant,<sup>7,20</sup> but an absolute evaluation would be needed to rigorously demonstrate that they can be ignored. Also there are a number of complicated additional terms which have not been accounted for. Terms responsible for compound-nucleus formation are conceptually grouped in this category.

Failure of the PWBA term to vary as indicated in Eq. (1) might be brought about by a "unitarity limiting" process. Effects of such a limitation have been considered previously in other contexts.<sup>6</sup> In the present reaction the limiting could come about if the first term of Eq. (1) yields a cross section which exceeds the unitarity limit for any of the few partial waves which can contribute appreciably in the incoming channel at low deuteron energy. A partial-wave decomposition of the experimental angular distribution, needed to verify this assumption, would seem to be difficult to interpret for low partial waves.<sup>37</sup> The observed bland angular distributions for this reaction,<sup>3</sup> if interpreted as arising only from the first term of Eq. (1), must be mainly due to low partial waves.

#### ACKNOWLEDGMENTS

We wish to express our appreciation for several helpful discussions with Professor J. M. Eisenberg and Professor D. Robson, and for the calculations and explanations of Dr. G. R. Satchler. John Stone has helped in the experiment and in some of the data analysis.

<sup>37</sup> See, e.g., J. Bowcock, Proc. Phys. Soc. (London) **A68**, 512 (1955).